Monte Carlo simulations of dose enhancement around gold nanoparticles used as X-ray imaging contrast agents and radiosensitizers

W. B. Li^{*a}, M. Müllner^a, M. B. Greiter^a, C. Bissardon^{a,b}, W. Z. Xie^{a,c}, H. Schlattl^a, U. Oeh^a, J. L. Li^c, C. Hoeschen^a

^aResearch Unit Medical Radiation Physics and Diagnostics, Helmholtz Zentrum München GmbH, Neuherberg, Germany; ^bDepartment of Physics, Claude Bernard University Lyon 1, Lyon, France; ^cDepartment of Engineering Physics, Tsinghua University, Beijing, China

ABSTRACT

Gold nanoparticles (GNPs) were demonstrated as X-ray imaging contrast agents and radiosensitizers in mice. However, the translational medical applications of GNPs in to the clinical practice need further detailed information on the biological effects related to the enhanced doses in malignant and healthy cells. The idea of improving radiotherapy with high atomic number materials, especially gold foils, was initiated in our research unit in the 1980s. Recently, experimental and theoretical efforts were made to investigate the potential improvement of imaging and radiotherapy with GNPs. Initially, the present work attempts to validate the dose enhancement effects of GNPs to cancer cells; secondly, it intends to examine the possible side effects on healthy cells when using GNPs as X-ray contrast agent. In this study, three Monte Carlo simulation programs, namely PENELOPE-2011, GEANT4 and EGSnrc were used to simulate the local energy deposition and the resulting dose enhancement of GNPs. Diameters of the GNPs were assumed to be 2 nm, 15 nm, 50 nm, 100 nm and 200 nm. The X-ray energy spectra for irradiation were 60 kVp, 80 kVp, 100 kVp, 150 kVp with a filtering of 2.7 mm Al for projectional radiography, and 8 mm Al for 100 kVp and 150 kVp for computed tomography. Additional peak energy of 200 kVp was simulated for radiotherapy purpose. The information of energy deposition and dose enhancement can help understanding the physical processes of medical imaging and the implication of nanoparticles in radiotherapy.

Keywords: Gold nanoparticle, dose enhancement, X-ray, medical imaging, radiotherapy, nanodosimetry.

1. INTRODUCTION

Since the late 1940s, the phenomenon of dose enhancement at interfaces between high and low atomic number (Z) materials has been an attractive scientific topic (Spiers 1949). Later in the 1980s, the concept of using high-Z materials for dose enhancement in cancer radiation therapy has been put forward (Matsudaira et al. 1980), which stimulated many scientific researchers in this field. As a high-Z material, gold has long been arisen the attention of researchers; however, it was until the last 15 years that gold was demonstrated to be used as radiosensitizer in radiation therapy and as X-ray contrast agent (Douglass et al. 2013). In the study of Regulla et al. (1998), fibroblast monolayers on a gold foil were irradiated by X-rays, inducing a physical dose enhancement factor of about 100 within a range of 10 micrometers and a biological enhancement factor of up to 50. Herold et al. (2000) injected gold microspheres with diameters between 1.5 -3.0 micrometers into a tumor followed by irradiation, and found that excised cells had reduced plating efficiency. Gold nanoparticles were applied as in vivo radiosensitizer for the first time by Hainfeld et al. (2004), who demonstrated that the GNPs did accumulate in tumors leading to a better radio-therapeutic result. Later on, the same group demonstrated that GNPs were useful X-ray contrast agents, as they showed that GNPs had no toxic effects and enabled higher contrast as well as longer imaging acquisition time (Hainfeld et al. 2006; 2008; 2011; 2012). Thereafter, more experimental work was focused on GNPs (Butterworth et al. 2008; Brun et al. 2009; Rahman et al. 2009; Liu et al. 2010). However differences among the experimental results imply that the radiosensitization of GNPs can be sensitive to the experimental conditions, for instance, irradiation parameters, particle sizes and GNP distribution in cells (Lechtman et al.

Medical Imaging 2014: Physics of Medical Imaging, edited by Bruce R. Whiting, Christoph Hoeschen, Despina Kontos, Proc. of SPIE Vol. 9033, 90331K ⋅ © 2014 SPIE ⋅ CCC code: 1605-7422/14/\$18 ⋅ doi: 10.1117/12.2043687

^{*}wli@helmholtz-muenchen.de; phone 0049 89 3187 3314; fax 0049 89 3187 2517; helmholtz-muenchen.de

2011). Monte Carlo simulations are another way to study the dose enhancement effect of GNPs with respect to different experimental conditions (Cho 2005; Cho et al. 2009; Jones et al. 2010; Leung et al. 2011; Chow et al. 2012; McMahon et al. 2011; Lechtman et al. 2013, Zygmanski et al. 2013). These researchers investigated mostly the dose enhancement of GNPs of various geometries and irradiation conditions at the microscopic scale. However, the clinical use of GNPs in molecular imaging and radiotherapy needs further information on the local energy deposition in the nanometer scale to assess the radiation dose effects, adverse effects on blood cells, immune cells and endothelial cells, even on DNA molecules due to the aptamer-conjugated nanoparticles; or for the intended radiotherapy effects on cancer cells.

The idea of using high-Z materials, especially gold foils to enhance radiotherapy was initiated in our research unit early in the 1980s (Regulla and Leischner 1983; Regulla et al. 1998; 2000; 2001; 2002). Recently, experimental and theoretical efforts have been made to investigate the potential improvement of medical imaging and radiotherapy with GNPs. In the present work, we attempt initially to validate the dose enhancement effects of GNPs to cancer cells; secondly we intend to examine the possible side effects on healthy cells when using GNPs as X-ray contrast agent. Three different Monte Carlo simulation programs, namely PENELOPE-2011, GEANT4 and EGSnrc, are used to simulate the local energy deposition and dose enhancement of secondary electrons in nanometer to micrometer ranges around nanoparticles of different sizes which are irradiated by X-rays with different peak voltages.

2. METHODS

Two Monte Carlo simulation codes, PENELOPE-2011 (Salvat et al. 2011) and GEANT4 (Agostinelli et al. 2003; Apostolakis et al. 2009), were used to simulate the secondary electron energy spectra, local energy deposition and the dose enhancement around GNPs in nanometer and micrometer ranges. The computer code system PENELOPE performs Monte Carlo simulations of coupled electron-photon transport in arbitrary materials for a wide energy range, from 50 eV to about 1 GeV. PENELOPE-2011 in its present form is the result of continued evolution from the first version, which was released in 1996. The program GEANT4 is a general Monte Carlo simulation toolkit for the simulation of particle-matter interactions in various research areas. Recently, GEANT4 has been extended to handle microdosimetry applications of very-low-energy particles in microscopic scale, and the corresponding new physical process modules have been included into a relatively independent program – the GEANT4-DNA project (Chauvie et al. 2006; 2007; Incerti et al. 2010, Francis et al. 2011). In order to track low-energy particles, say less than 100 eV, in the nanometer dimensions, the newly implemented GEANT4-DNA physical process modules and the standard electromagnetic processes were applied.

The simulation geometry is illustrated in Figure 1. A single GNP sphere was positioned at the center of the simulation tracking volume consisting of liquid water. The GNP was irradiated by parallel X-ray beams, the axis of which was aligned to the center of the GNP. The X-ray beams were emitted from a circular plane source located 1 mm away from the center, and they were all parallel with the central axis. The circular plane source was assumed to be the same diameter as the corresponding GNP for an increase of the interaction probability of the X-ray beams and the GNP. To score the dose enhancement around the GNP, the surrounding water was divided into several shells. Starting from the surface of the GNP, 20 water shells with the same thickness of 1 µm were set as sensitive target volumes. In addition, doses in another 20 water shells with the trackings volume, different quantities, e.g. original position, energy and momentum, the physical process and the deposited energy of each interaction can be stored for further analysis. In the present work, the average total deposited energy within each water shell was recorded. To estimate the dose enhancement effect, another group of simulations, in the same geometry condition but without gold nanoparticles in liquid water, were also carried out. The dose enhancement factor (DEF) was defined as the ratio of the average doses within the same target water shell resulting from X-ray irradiation with and without GNP in the liquid water.

In PENELOPE-2011 simulations, the diameters of the GNPs were assumed as 2 nm, 15 nm, 50 nm, 100 nm and 200 nm, and the X-ray peak voltages were 60 kVp, 80 kVp, 100 kVp, 150 kVp with filtering of 2.7 mm Al for projectional radiography, and 8 mm Al for 100 kVp and 150 kVp for computed tomography (CT). Additional peak energy of 200 kVp was performed only for radiotherapy purpose. For a preliminary comparison, in GEANT4 simulations, 2 nm, 50 nm and 100 nm were chosen to be representative diameters of GNPs, together with 60 kVp and 100 kVp to be representative X-ray peak voltages.

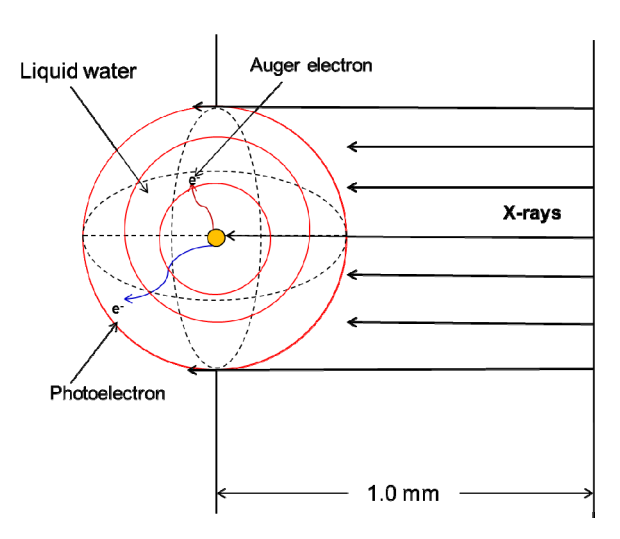


Figure 1. Schematic diagrams of the simulation geometry for PENELOPE-2011 and GEANT4 programs.

Furthermore, the Monte Carlo program EGSnrc (Kawrakow and Rogers 2000) was used to simulate the dose enhancement in liver tissue containing different amounts of gold. GNPs were not explicitly modeled in these simulations; instead a homogeneous distribution of gold in the tissue was modeled. For the simulations X-rays with peak voltages of 60 kVp, 80 kVp, 100 kVp, 120 kVp and 140 kVp were used.

3. RESULTS

In this section, the simulated dose enhancement factors (DEFs) in the micrometer and nanometer ranges around GNPs of different diameters irradiated by various X-rays are presented. The simulation results of PENELOPE-2011 are presented in Figures 2 - 5, while the results of GEANT4 are shown in Figures 6 - 9. The results are presented in two categories: one for the DEF curves of GNPs with different diameters but the same X-ray peak voltages, the other for those of different X-ray peak voltages with the same GNP diameters. Note that all the values shown at the zero point of X-axis denote the DEFs inside the GNPs. The DEFs inside the 2 nm sphere nanoparticle were not calculated, as the deposited energy in this tiny water sphere can hardly be recorded.

In the framework of simulation using EGSnrc code, the dose enhancement in liver tissue containing different amounts of gold which was homogeneously distributed in the tissue, and the dose enhancement in the micrometer range in the vicinity of a gold foil of 1 μ m thickness are shown in Figure 10.

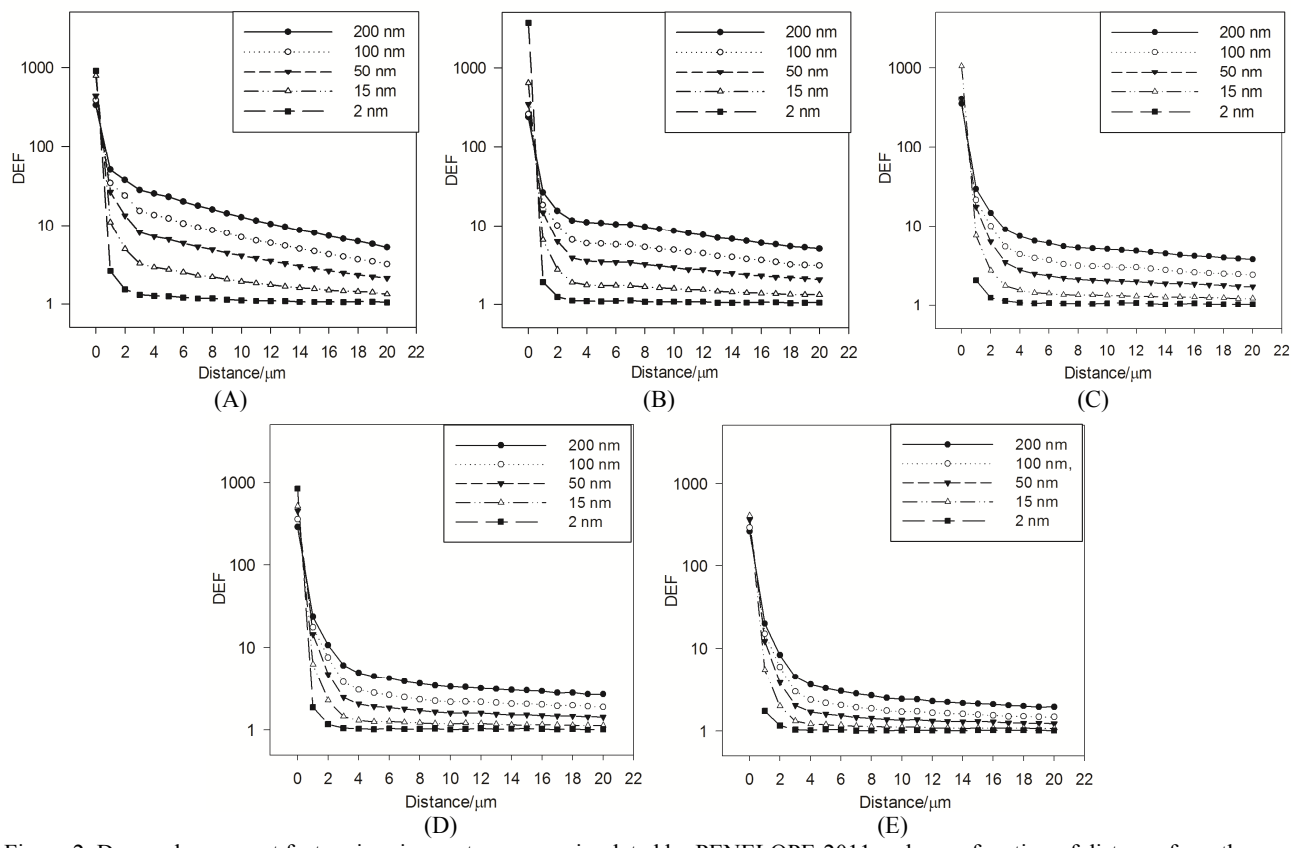


Figure 2. Dose enhancement factors in micrometer ranges simulated by PENELOPE-2011 code as a function of distance from the surface of the GNPs. GNPs were irradiated by X-rays with peak voltages of 60 kVp (A), 80 kVp (B), 100 kVp (C), 150 kVp (D) and 200 kVp (E).

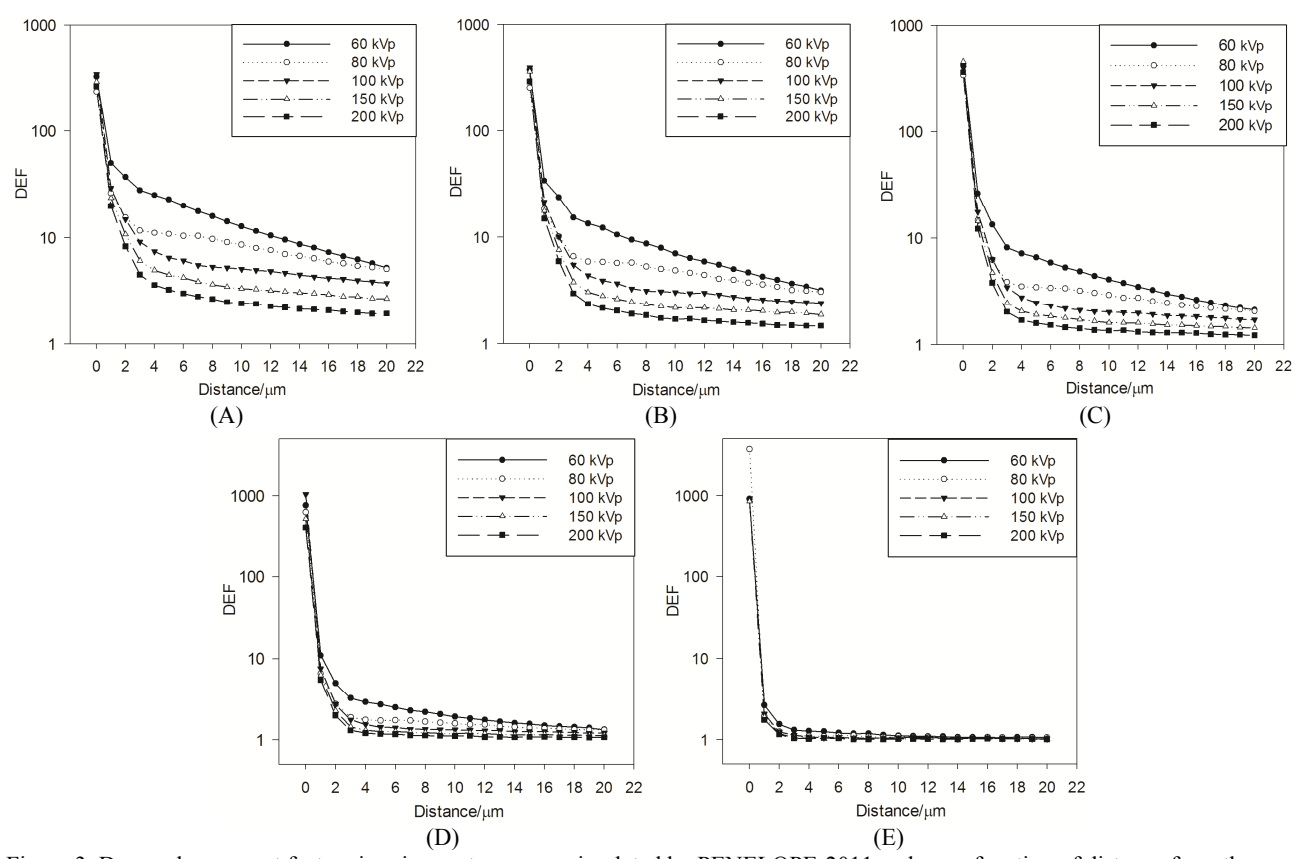


Figure 3. Dose enhancement factors in micrometer ranges simulated by PENELOPE-2011 code as a function of distance from the surface of the GNP. Diameters of GNPs were 200 nm (A), 100 nm (B), 50 nm (C), 15 nm (D) and 2 nm (E).

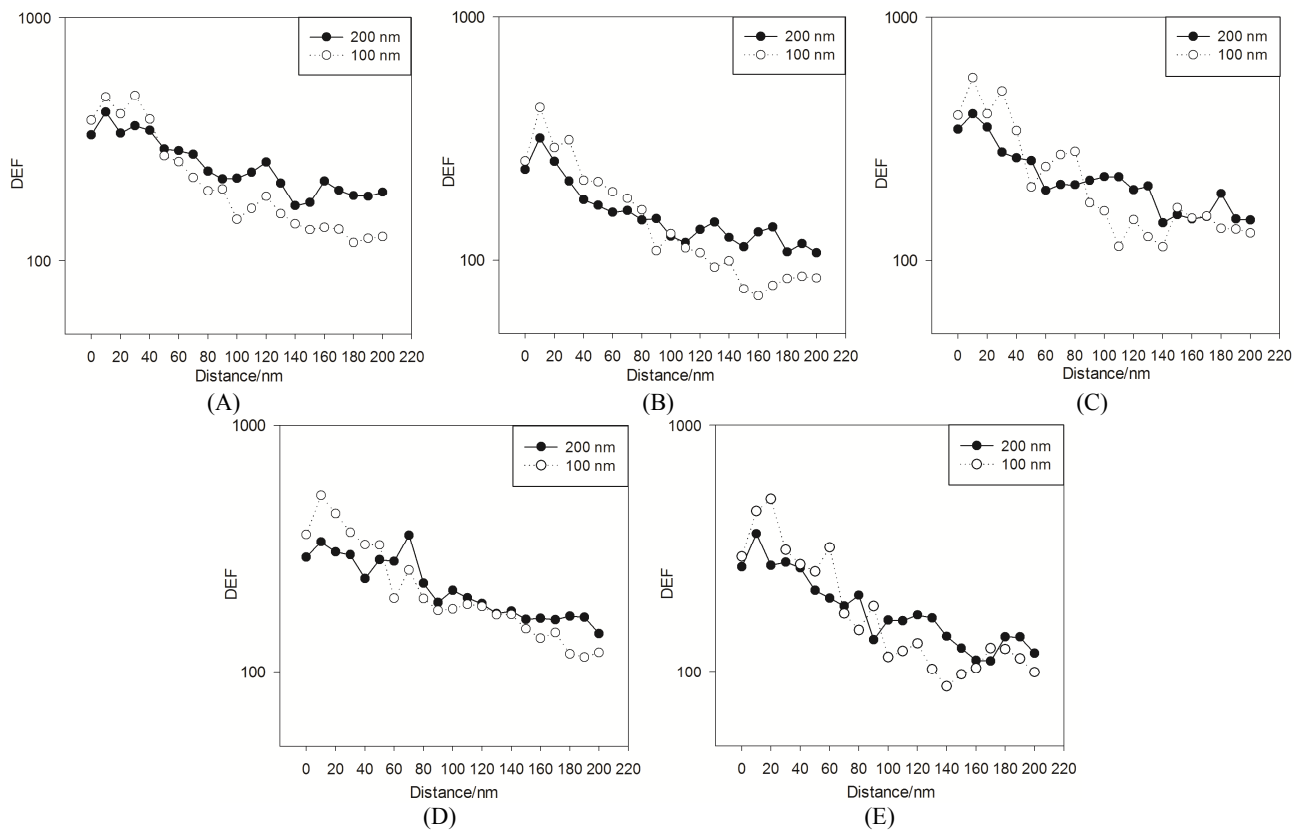


Figure 4. Dose enhancement factors in nanometer ranges simulated by PENELOPE-2011 code as a function of distance from the surface of the GNPs. GNPs were irradiated by X-rays with peak voltages of 60 kVp (A), 80 kVp (B), 100 kVp (C), 150 kVp (D) and 200 kVp (E).

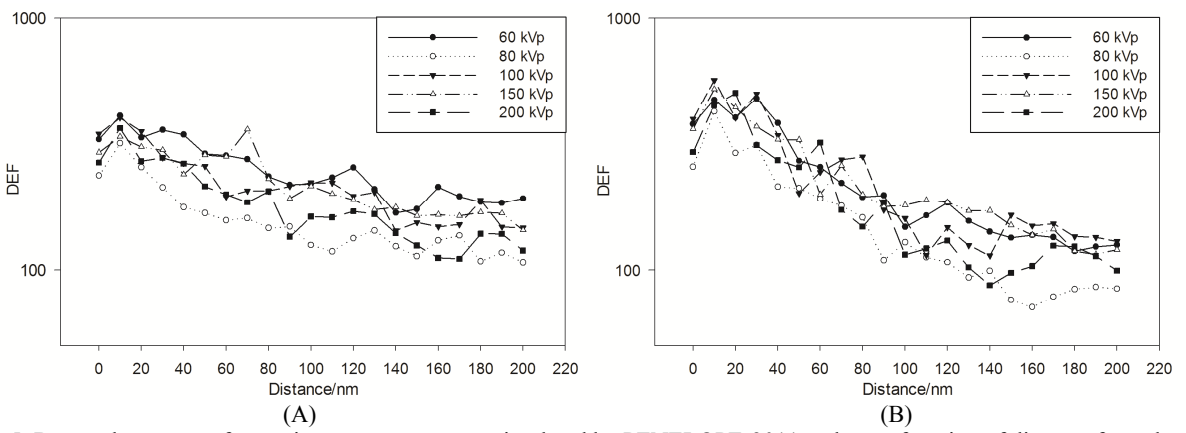


Figure 5. Dose enhancement factors in nanometer ranges simulated by PENELOPE-2011 code as a function of distance from the surface of the GNPs. Diameters of GNPs were 200 nm (A) and 100 nm (B).

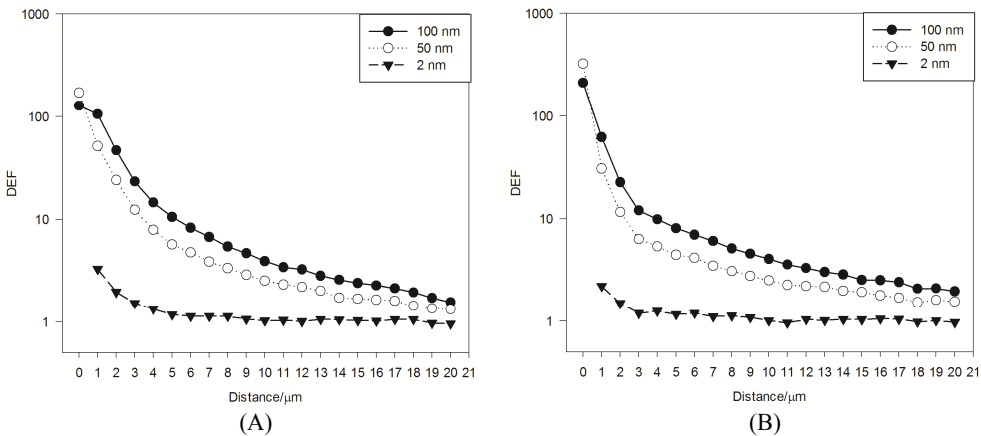


Figure 6. Dose enhancement factors in micrometer ranges simulated by GEANT4 as a function of distance from the surface of the GNPs. GNPs were irradiated by X-rays with peak voltages of 60 kVp (A) and 100 kVp (B).

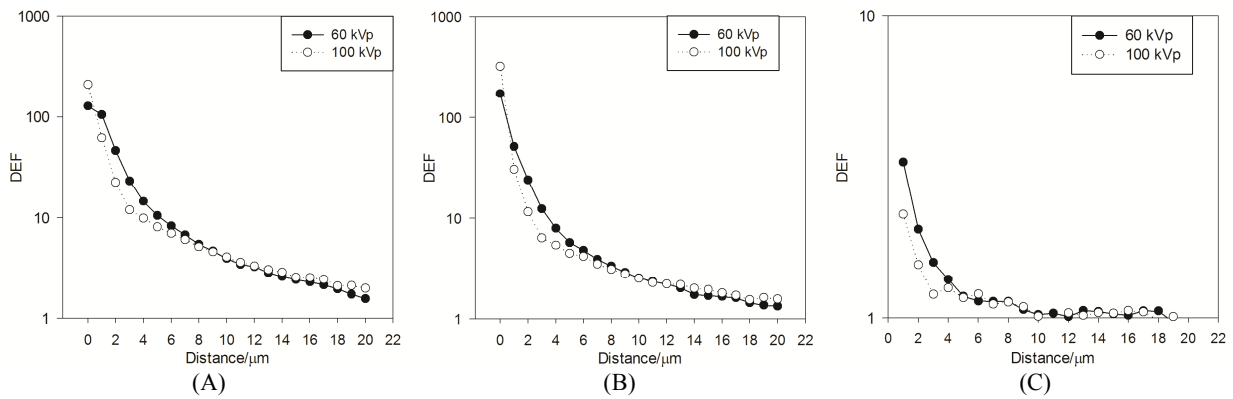


Figure 7. Dose enhancement factors in micrometer ranges simulated by GEANT4 code as a function of distance from the surface of the GNPs. Diameters of GNPs were 100 nm (A), 50 nm (B) and 2 nm (C).

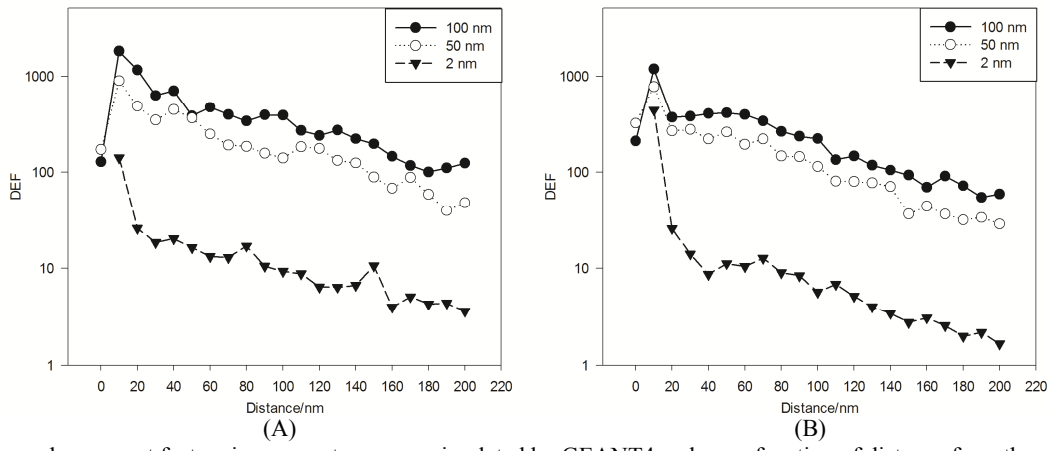


Figure 8. Dose enhancement factors in nanometer ranges simulated by GEANT4 code as a function of distance from the surface of the GNPs. GNPs were irradiated by X-rays with peak voltages of 60 kVp (A) and 100 kVp (B).

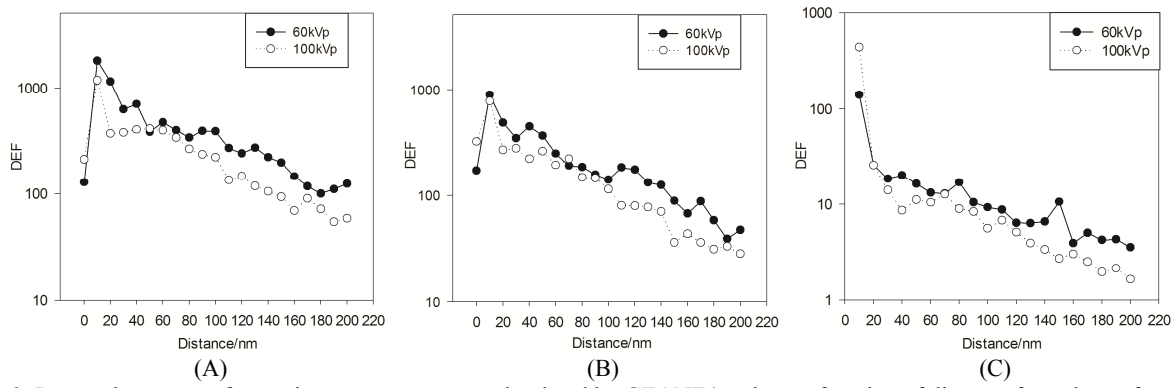


Figure 9. Dose enhancement factors in nanometer ranges simulated by GEANT4 code as a function of distance from the surface of the GNPs. Diameters of GNPs were 100 nm (A), 50 nm (B) and 2 nm (C).

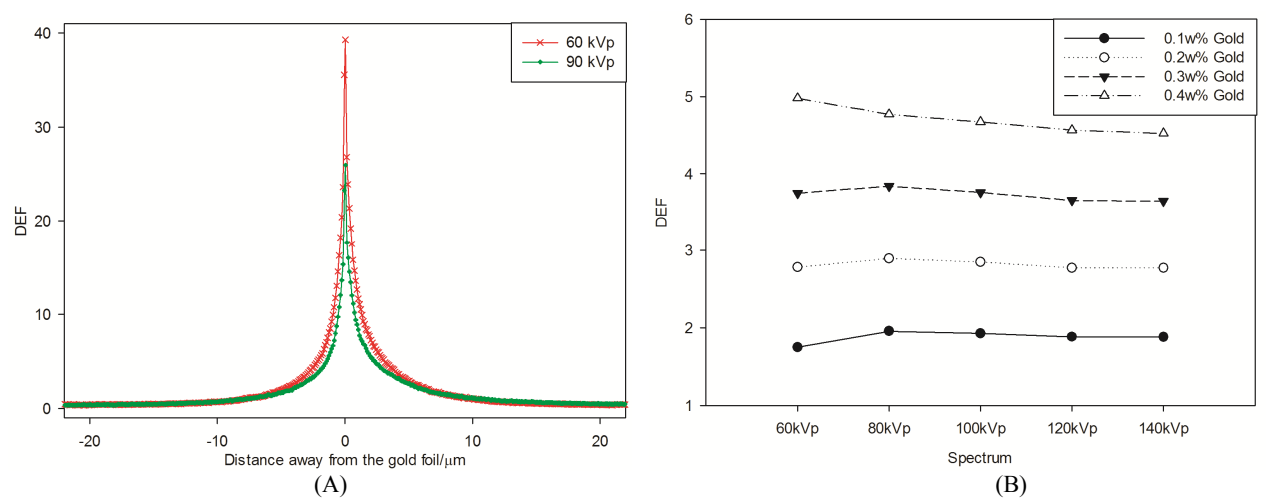


Figure 10. Dose enhancement factors forwards and backwards from a gold foil of 1 µm thickness irradiated by X-rays with energy spectra of 60 kVp and 90 kVp which are simulated by EGSnrc code (A). Dose enhancement factor simulated by using EGSnrc code for different X-ray spectra and different amounts of gold homogeneously distributed in liver tissue (B).

4. DISCUSSIONS

As shown in Figures 2, 3, 6 and 7, the simulated DEFs in micrometer ranges around GNPs decline with increasing distance from the surface of the GNPs. DEFs of the first 2 - 3 inner water shells decrease much more rapidly than those of outer water shells.

When GNPs in different diameters were irradiated by the same peak voltage X-rays, the DEFs of the first 1 μ m water shells decrease as the diameters of GNPs decrease. The DEFs for GNPs of diameter of 2 nm are especially small with a maximum value of 5 in the first 1 μ m water shell, while the corresponding DEFs of GNPs with other diameters reach up to several tens. This might be due to interactions of X-rays and GNPs, which produce sufficient secondary electrons and Auger electrons and cause more energy deposition and the consequential dose enhancement effect in the immediate volume around gold.

For GNPs in the same diameter irradiated by X-rays with different peak voltages, some differences in simulated DEFs are observed between PENELOPE-2011 and GEANT4 codes. Figure 3 shows results simulated by PENELOPE-2011 code. In the first 1 µm water shells, DEFs of GNPs with 200 nm, 100 nm and 50 nm decrease obviously with increasing

peak voltages. For GNPs with 15 nm diameter, the DEF curve of 60 kVp distinguishes from the others; while for GNPs with 2 nm diameter, the DEF curves are in a similar level. The results simulated by GEANT4 code are shown in Figure 7. For GNPs with 100 nm and 50 nm diameters, the DEFs of 60 kVp are larger than those of 100 kVp before the 9th - 10th water shells, after 10th water shell, the DEFs become relatively small and stay in the similar level.

The DEFs in nanometer ranges around GNPs are plotted in Figure 4, 5, 8 and 9. Generally, the DEFs decline, in a manner of fluctuation, as the distances from the GNP surface increase. It might be due to the statistical property and simulation numbers in the nanometer ranges, it will be investigated in the current ongoing work. In addition, the highest DEF values of all the curves in nanometer ranges, mostly in the first 10 nm water shell, are usually a few hundreds, and are about 10 times larger than those in micrometer ranges. This significant dose enhancement effect might be attributed to the low-energy Auger electrons, whose effective ranges were limited within several tens to hundreds of nanometers.

Taking all the simulation results into account, 60 kVp seems to be the specific peak voltage of X-ray that leads to the greatest dose enhancement effect for GNPs. Moreover, for the same X-ray irradiation, the larger the GNP is, the stronger is the dose enhancement effect which will be achieved. However, when using GNPs as X-ray imaging contrast agents or radiosensitizers, other biological factors must be taken into consideration for choosing the optimized size of GNP.

It should be pointed out that there are differences between the simulation results of PENELOPE-2011 and GEANT4. Detailed energy spectra of secondary electrons deposited in the water shells in micrometer and nanometer ranges are needed to be analyzed and compared thoroughly in the continuing work.

The simulated DEF of 40, by using EGSnrc code, in the 1 µm shell from the 1 µm gold foil is comparable to the DEF of 50 gained from the results simulated by PENELOPE-2011 code, however, considerably lower than the value of 105 obtained from simulation by GEANT4 code, in the first 1 µm shell obtained for GNPs for the same X-ray of 60 kVp, respectively (Figures 3A, 7A and 10A). For the results of different X-ray spectra and different amounts of gold homogeneously distributed in liver tissue simulated by EGSnrc code, the dose enhancement factors are almost independent of the used irradiated spectra. The amount of gold is the main factor influencing the dose enhancement. For 0.1w% gold the maximum dose enhancement factor is 2 at 80 kVp, 3 at 80 kVp for 0.2w% gold, 4 at 80 kVp for 0.3w% gold and 5 at 60 kVp for 0.4w% gold (Figure 10B).

One aspect of limitations of the Monte Carlo transport simulations of very-low-energy electrons/photons should be addressed. Both of the Monte Carlo simulation programs, PENELOPE-2100 and GEANT4, provide event-by-event transports of particles in material down to 50 eV, even to several eV in GEANT4-DNA. The low-energy electrons are important for simulations of dose enhancement effects in the micrometer and nanometer ranges. However, as pointed out by Thomson and Kawrakow (2011), in order to satisfy the Heisenberg uncertainty principle, uncertainties of 5% must be assigned to position and momentum for 1 keV electrons in water; at 100 eV, these uncertainties are 17 to 20% and are even larger at lower energies, for example, 50 eV in the present study. Therefore a large uncertainty of the dose enhancement factor simulated in the nanometer range should be preconceived.

5. CONCLUSIONS

In the present work, the dose enhancement factors around GNPs irradiated by X-rays in different irradiation scenarios are simulated and compared within three MC simulation programs in our research unit. Generally, the DEFs in both micrometer and nanometer ranges decrease with increasing distance from the surface of GNPs, however, the maximum DEFs in nanometer ranges can be ten times larger than those in micrometer ranges. Among X-rays with different peak voltages, 60 kVp seems to be the specific one, which leads the greatest dose enhancement effect for GNPs in different sizes.

In addition, stronger dose enhancement effects appear around the GNP with a larger size, when irradiated by X-rays with the same energy peak voltage. Auger electrons contribute to the DEFs at the nanometer ranges, whereas other secondary electrons to the micrometer ranges. The higher dose enhancements in nanometer range around the nanoparticles support the potential application of GNPs in the targeted gene radiotherapy (Foley et al. 2005; Farokhzad et al. 2006; Yang et al. 2011).

It is noted that, for the same geometry set-up and X-rays with the same peak voltage, a difference of a factor of 2 for DEFs simulated by the two programs, PENELOPE-2011 and GEANT4, is observed. A further detailed analysis of the

secondary electron energy spectra in and around the GNPs is currently being carried out in order to reach a higher quality assurance in radiation transport simulations with different Monte Carlo programs.

REFERENCES

- [1] Agostinelli S. et al. Geant4 A simulation toolkit. Nucl. Instrum. Methods. Phys. Res. A. 506: 250-303 (2003).
- [2] Apostolakis J. et al. Geometry and physics of the Geant4 toolkit for high and medium energy applications. Radiat. Phys. Chem. 78: 859-873 (2009).
- [3] Brun E, Sanche L, Sicard-Roselli C. Parameters governing gold nanoparticle X-ray radiosensitization of DNA in solution. Colloids. Surf. B. 72: 128-134 (2009).
- [4] Butterworth KT, Wyer JA, Brennan-Fournet M, Latimer CJ, Shah MB, Currell FJ, Hirst DG. Variation of strand break yield for plasmid DNA irradiated with high-Z metal nanoparticles. Radiat. Res. 170: 381-387 (2008).
- [5] Chauvie S, Francis Z, Guatelli S, Incerti S, Mascialino B, Montarou G, Moretto Ph, Nieminen P, Pia MG. Monte Carlo simulation of interactions of radiation with biological systems at the cellular and DNA levels: The Geant4-DNA Project. Radiat. Res. 166: 676-677 (2006).
- [6] Chauvie S, Francis Z, Guatelli S, Incerti S, Mascialino B, Moretto P, Nieminen P, Pia MG. Geant4 physics processes for microdosimetry simulation: design foundation and implementation of the first set of models. IEEE Trans. Nucl. Sci. 54: 2619-2628 (2007).
- [7] Cho SH, Jones BL, Krishnan S. The dosimetric feasibility of gold nanoparticle-aided radiation therapy (GNRT) via brachytherapy using low-energy gamma-/x-ray sources. Phys. Med. Biol. 54: 4889-4905 (2009).
- [8] Cho SH. Estimation of tumour dose enhancement due to gold nanoparticles during typical radiation treatments: a preliminary Monte Carlo study. Phys. Med. Biol. 50: N163-N173 (2005).
- [9] Chow JC, Leung MK, Jaffray DA. Monte Carlo simulation on a gold nanoparticle irradiated by electron beams. Phys. Med. Biol. 57: 3323-3331 (2012).
- [10] Douglass M, Bezak E, Penfold S. Monte Carlo investigation of the increased radiation deposition due to gold nanoparticles using kilovoltage and megavoltage photons in a 3D randomized cell model. Med. Phys. 40, 071710 (2013); doi: 10.1118/1.4808150.
- [11] Farokhzad OC, Karp JM, Langer R. Nanoparticle–aptamer bioconjugates for cancer targeting. Expert Opin. Drug Deliv. 3(3): 311-324 (2006).
- [12] Foley EA, Carter JD, Shan F, Guo T. Enhanced relaxation of nanoparticle-bound supercoiled DNA in X-ray radiation. Chem. Commun. 25: 3192-3194 (2005).
- [13] Francis Z, Incerti S, Capra R, Mascialino B, Montarou G, Stepan V, Villagrasa C. Molecular scale track structure simulations in liquid water using the Geant4-DNA Monte-Carlo processes. Appl. Radiat. Isot. 69: 220-226 (2011).
- [14] Hainfeld JF, Dilmanian FA, Slatkin DN, Smilowitz HM. Radiotherapy enhancement with gold nanoparticles. J. Pharm. Pharmacol. 60 (8): 977-985 (2008).
- [15] Hainfeld JF, O'Connor MJ, Dilmanian FA, Slatkin DN, Adams DJ, Smilowitz HM. Micro-CT enables microlocalisation and quantification of Her2-targeted gold nanoparticles within tumour regions. Br. J. Radiol. 84 (1002): 526-533 (2011).
- [16] Hainfeld JF, Slatkin DN, Focella TM. Smilowitz HM. Gold nanoparticles: a new X-ray contrast agent. Br. J. Radiol. 79: 248-253 (2006).
- [17] Hainfeld JF, Slatkin DN, Smilowitz HM. The use of gold nanoparticles to enhance radiotherapy in mice. Phys. Med. Biol. 49: N309-N315 (2004).
- [18] Hainfeld JF, Smilowitz HM, O'Connor MJ, Dilmanian FA, Slatkin DN. Gold nanoparticle imaging and radiotherapy of brain tumors in mice. Nanomedicine (Lond). 8 (10): 1601-1609 (2013).
- [19] Herold DM, Das IJ, Stobbe CC, Iyer RV, Chapman JD. Gold microspheres: a selective technique for producing biologically effective dose enhancement. Int. J. Radiat. Biol. 76: 1357-1364 (2000).

Proc. of SPIE Vol. 9033 90331K-10

- [20] Incerti S, Baldacchino G, Bernal M, Capra R, Champion C, Francis Z, Guatelli S, Guèye P, Mantero A, Mascialino B, Moretto P, Nieminen P, Rosenfeld A, Villagrasa C, Zacharatou C. The Geant4-DNA project. Int. J. Model. Simul. Sci. Comput. 1: 157-178 (2010).
- [21] Jones BL, Krishnan S, Cho SH. Estimation of microscopic dose enhancement factor around gold nanoparticles by Monte Carlo calculations. Med. Phys. 37(7): 3809-3816 (2010).
- [22] Kawrakow I, Rogers DWO. The EGSnrc code system: Monte Carlo simulation of electron and photon transport. Technical Report PIRS-701. Ottawa, Canada: National Research Council of Canada, 2000.
- [23] Lechtman E, Chattopadhyay N, Cai Z, Mashouf S, Reilly R, Pignol JP. Implications on clinical scenario of gold nanoparticle radiosensitization in regards to photon energy, nanoparticle size, concentration and location. Phys. Med. Biol. 56: 4631-4647 (2011).
- [24] Lechtman E, Mashouf S, Chattopadhyay N, Keller BM, Lai P, Cai Z, Reilly RM, Pignol JP. A Monte Carlobased model of gold nanoparticle radiosensitization accounting for increased radiobiological effectiveness. Phys. Med. Biol. 58: 3075-3087 (2013).
- [25] Leung MK, Chow JC, Chithrani BD, Lee MJ, Oms B, Jaffray DA. Irradiation of gold nanoparticles by X-rays: Monte Carlo simulation of dose enhancements and the spatial properties of the secondary electrons production. Med. Phys. 38(2): 624-631 (2011).
- [26] Liu CJ et al. Enhancement of cell radiation sensitivity by pegylated gold nanoparticles. Phys. Med. Biol. 55: 931-945 (2010).
- [27] Matsudaira H, Ueno AM, Furuno I. Iodine contrast medium sensitizes cultured mammalian cells to X-rays but not to γ rays. Radiat. Res. 84: 144-148 (1980).
- [28] McMahon SJ et al. Biological consequences of nanoscale energy deposition near irradiated heavy atom nanoparticles. Scientific Reports. (2011); doi: 10.1038/srep00018.
- [29] Rahman WN, Bishara N, Ackerly T, He CF, Jackson P, Wong C, Davidson R, Geso M. Enhancement of radiation effects by gold nanoparticles for superficial radiation therapy. Nanomedicine. 5: 136-142 (2009).
- [30] Regulla D, Friedland W, Hieber L, Panzer W, Seidenbusch M Schmid E. Spatially limited effects of dose and LET enhancement near tissue/gold interfaces at diagnostic X ray qualities. Radiat. Prot. Dosim. 90 (1-2): 159-163 (2000).
- [31] Regulla D, Hieber L, Seidenbusch M. Physical and biological interface dose effects in tissue due to X-ray-induced release of secondary radiation from metallic gold surfaces. Radiat. Res. 150: 92-100 (1998).
- [32] Regulla D, Panzer W, Schmid E. Stephan G, Harder D. Detection of Elevated RBE in human lymphocytes exposed to secondary electrons released from X-irradiated metal surfaces. Radiat. Res. 155: 744-747 (2001).
- [33] Regulla D, Schmid E, Friedland W, Panzer W, Heinzmann U, Harder D. Enhanced values of the RBE and H ratio for cytogenetic effects induced by secondary electrons from an X-irradiated gold surface. Radiat. Res. 158: 505-515 (2002).
- [34] Regulla DF, Hieber LB, Seidenbusch M. Physical and biological interface dose effects in tissue due to X-Ray-induced release of secondary radiation from metallic gold surfaces. Radiat. Res. 150: 92-100 (1998).
- [35] Regulla DF, Leischner U. Comparing interface dosimetry with conventional methods and TSEE. Radiat. Prot. Dosim. 4 (3-4): 174-176 (1983).
- [36] Salvat F, Fernandez-Valrea JM, Sempau J. Penelope-2011: A code system for Monte Carlo simulation of electron and photon transport. OECD Nuclear Energy Agency, Issy-les-Moulineaux, 2011.
- [37] Spiers FW. The influence of energy absorption and electron range on dosage in irradiated bone. Br. J. Radiol. 22: 521-533 (1949).
- [38] Thomson RM and Kawrakow I. On the Monte Carlo simulation of electron transport in the sub-1 keV energy range. Med. Phys. 38(8): 4531-4534 (2011).
- [39] Yang L, Zhang X, Ye M, Jiang J, Yang R, Fu T, Chen Y, Wang K, Liu C, Tan W. Aptamer-conjugated nanomaterials and their applications. Adv. Drug. Deliv. Rev. 63 (14-15): 1361-1370 (2011).
- [40] Zygmanski P, Liu B, Tsiamas P, Cifter F, Petersheim M, Hesser J, Sajo E. Dependence of Monte Carlo microdosimetric computations on the simulation geometry of gold nanoparticles. Phys. Med. Biol. 58 7961-7977 (2013).